Molecular Dynamics Simulations of Pd Deposition on the α-Al_2O_3 (0001) Surface

Norge Cruz Hernández and Javier Fernandez Sanz*

Departamento de Química Física, Facultad de Química, E-41012, Sevilla, Spain

Received: August 7, 2001; In Final Form: October 8, 2001

Molecular dynamics simulations of Pd clusters supported on the undefective α-Al_2O_3 (0001) surface are reported. The alumina surface is represented by a slab obtained by imposing periodic boundary conditions to a $4 \times 4 \times 2$ supercell. The dynamics of the system is accounted for through classical pair potentials describing both the metal−metal and the metal-surface interactions and have been derived from periodic density functional theory model calculations. Deposited particles show a well defined structure and can be described as truncated pyramids mainly exhibiting (111) facets in agreement with recent scanning tunnel microscopy experiments conducted under atomic resolution. These particles show stability at moderate temperatures (up to ∼400 K), but when the system is heated ($T = 500$ K), Pd atoms leave the surface and diffuse into the bulk. Such a diffusion would be in agreement with the loose of activity observed in Pd/Al_2O_3/NiAl(110) catalysts when the temperature is raised beyond 500 K.

I. Introduction

Understanding the nature of transition-metal/metal-oxide interfaces constitutes one of the most appealing challenges nowadays for material scientists. These metal−ceramic based materials play a significant role in photolysis and photooxidation reactions, electrocatalysis, gas sensors, catalysis by supported metals, etc.[1−3] Because of both its mechanical and thermal resistance, aluminum oxide is one of the most widely used supports for catalysis purposes. Aluminum oxide is also of special interest in the experimental modeling of catalysts because of the well ordered surfaces that can be prepared from oxidation of NiAl(110) crystals.[4] Defectiveness of these surfaces has been carefully investigated.[5] Among transition metals, palladium exhibits a well-known ability to catalyze a large number of chemical reactions. The growth and structure of Pd deposits on Al_2O_3 have been studied over a wide range of conditions, and the results have been recently reviewed.[6,7] Scanning tunneling microscopy (STM) under atomic resolution showed the regular structure of Pd particles exhibiting a well-defined morphology of crystallites. The STM images revealed that Pd particles grow in (111) orientation, preferentially exposing (111) facets and only a small fraction of (100) facets.[8] Such epitaxially grown supported Pd particles constitute useful model catalysts whose activity has been investigated in several settings. For instance, the ability to adsorb CO and the kinetics of the subsequent oxidation have been reported,[9,10] as well as the photochemistry of adsorbed methane.[11] Concerning the growth of palladium clusters on the (0001) basal plane of the native oxide, both Volmer−Weber, VW,[12] (i.e., three-dimensional, 3D) and two-dimensional island[13] (2D-I) mechanisms have been proposed. More recently,[14] noncontact atomic force microscopy (NC-AFM) has been used to image the room-temperature growth of palladium and copper on the (1×1) and $[(31)^{1/2} \times (31)^{1/2}]R \pm 9°$ terminations of α-Al_2O_3 (0001). Three-dimensional islands of palladium were observed on both terminations, and a step-dominated growth, similar to the behavior on thin film Al_2O_3/NiAl(110), was found in the case of reconstructed surfaces.

The Pd/alumina interface has also been investigated from a theoretical point of view using modern quantum mechanical methods. Bogicevic et al.[15] reported a theoretical study based on the periodic density functional theory (DFT) and plane waves to span the electronic states. Using the local density approach (LDA), the adsorption energy for Pd on an Al_2O_3 film growth on Al(111) was found to be 3.2 eV. In a more recent work, we reported on ab initio embedded clusters and periodic DFT calculations of Pd atoms adsorbed on the (0001) facet of α-Al_2O_3.[16] Our periodic DFT calculations based on a generalized gradient approximation (GGA) showed that the preferred site is atop of surface oxygen atoms, with an adsorption energy of 1.41 eV. Our analysis also revealed that the Pd−surface interaction arises mainly from two contributions: a polarization of the transition metal caused by the surface electrostatic field and, to a lesser extent, some charge transfer from the Pd atoms toward the surface, in particular to the outermost Al atoms. As a direct consequence of such a reduction, there is a noticeable surface relaxation induced by the adsorbate involving mainly an outward displacement of the outermost aluminum atoms.

In the present paper, we report on a molecular dynamics (MD) classical simulations of the atomistic structure of a Pd particle supported on the α-Al_2O_3 (0001) surface. Our main goal is, first of all, to analyze the structure of the supported clusters in view of obtaining details of potentially active sites. Second, the stability of such deposits against temperature will be examined. This point is of major interest because it has been clearly demonstrated that the surface activity decreases upon heating, likely due to a diffusion of Pd atoms across the alumina films.[17,18] In contrast to ab initio MD of the type of Car−Parrinello based methods,[19] the present MD classical simulations permit the handling of medium sized deposited clusters consisting of several tens of atoms while simultaneously allowing the relaxation of both substrate and deposited cluster. In other words, this allows us to simulate systems of real size because it has been shown that under specific experimental conditions the deposits contain a few hundred atoms.[9] The computational procedure closely follows that recently employed in our group for the MD simulations of the MgO hydroxylation[20] and Pd adsorption[21] on MgO (0001), namely, the determination of surface−adsorbate and adsorbate−adsorbate pair potentials from a series of single-point periodic DFT model calculations (section

* To whom correspondence should be addressed. E-mail: sanz@cica.es.

10.1021/jp0130517 CCC: $20.00
Published on Web 11/07/2001

II) and MD simulations in a range of coverage and temperatures (section III). Finally, the conclusions will be outlined in section IV.

II. Determination of the Interaction Pair Potentials

The starting point in a classical MD simulation concerns the choice of the force field governing the behavior of the system. It is generally accepted that a simple and suitable description of a set of interacting particles can be achieved by means of additive pair potentials V_{ij}. Following the strategy previously reported,[20,21] two qualitatively different types of pair potentials were used in this work. The first accounts for the interaction between surface support species, i.e., between aluminum and oxygen ions, and the second accounts for the interaction between Pd atoms and surface ions, as well as between Pd atoms themselves. To describe the Al−O interaction, a typical pair potential built up as a sum of short- and long-range contributions was chosen:

$$V_{ij} = V_{ij}(s - r) + V_{ij}(l - r) \quad (1)$$

where the long-range term $V_{ij}(l - r)$ represents the Coulombic contribution $(q_i,q_j)/r_{ij}$, with q_i,q_j being the charge of species i,j (+3 and −2, for Al^{3+} and O^{2-}). The short-range potential $V_{ij}(s - r)$ used for Al^{3+} and O^{2-} ions was of the Buckingham type according to the expression

$$V_{ij}(s - r) = A_{ij} \exp(-B_{ij}r_{ij}) - C_{ij}/r_{ij}^{6} \quad (2)$$

where parameters A, B, and C were those optimized by Lewis and Catlow.[22] The reliability of this pair potential to reproduce the alumina surface properties has been previously reported.[23,24] Thus, the contraction of the first interlayer distance is −57.9%, in agreement with experiment (−51.2%).[25] Also the surface energy is estimated to be[23] 2.14 J/m^2, in agreement with that obtained from MM[26] (2.03 J/m^2), DFT[27,28] (2.00, 1.76 J/m^2), and MD with different potential[29] (2.04 J/m^2).

The pair potentials representing the interaction of Pd−O, Pd−Al, and Pd−Pd have been determined on a first-principles basis from GGA density functional calculations closely following the procedure initially proposed by Oviedo et al.[20] although a periodic approach is used in the present work as opposed to the use of embedded cluster models. The reason for this arises from the difficulty of describing both acidic and basic sites of a complex surface using an equivalent cluster model, i.e., in which border effects are equally balanced. Therefore, it seems safer for a systematic work to employ a periodic model. The price to pay is the need to deal with the adsorbate−adsorbate contribution arising from the intercell interaction. For the size of the cell used here, such interaction amounts to a tenth of an eV, which compared to the smallest adhesion energy (about 1 eV, for the on-top Al site) justifies a posteriori correction.

Periodic supercell 3D DFT calculations were carried out using the VASP 4.4.3 code.[30−32] The calculations were performed for a 1/3 ML Pd coverage, and the energy was obtained using the GGA implementation of DFT proposed by Perdew et al.[33] Ultrasoft pseudopotentials[34] were employed to remove the core electrons from the calculations, and a plane-wave basis set was used to span the valence electronic states. The cutoff energy for the plane waves was 337 eV and the Monkhorst−Pack set of four k points was used. A rhombic prism unit cell belonging to the hexagonal system was used to represent the surface, and a vacuum width of 10 Å was allowed between the slabs. To select the thickness of the slab, two different possibilities were considered: 18 and 12 layers (30 and 20 atoms per unit cell).

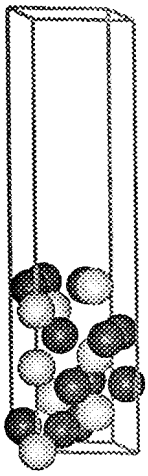

Figure 1. Supercell containing 20 atoms used to represent the surface in the periodic GGA calculations. Dark and light spheres correspond to oxygen and aluminum atoms, respectively.

The corresponding slabs were partially optimized allowing the top outermost six layers to relax. Variations of the interplanar distances for the outermost layers were found to be 0.118, 0.876, 0.259. and 1.016 Å for the 18 layer thick slab, and 0.118, 0.870, 0.266, and 1.011 Å for the 12 layer thick slab. Because the differences are almost negligible, the smaller 12 layer thick unit cell was chosen to represent the surface (see Figure 1). Moreover, it should be noticed that, in percentage terms, these values are virtually identical to those obtained from previous DFT calculations: first layer (Al), −86%; second layer (O), 4%; third layer (Al), −48%; fourth layer (Al), 21%.[35]

To model the interaction of a single palladium atom with the α-Al_2O_3 (0001) undefective surface, the acidic and basic adsorption sites were considered separately. The acidic site was represented by an Al terminated surface on which a single Pd atom was deposited on top of the outermost Al atom. In a similar way, the interaction with basic sites was described by depositing one Pd atom on top of oxygen of an O terminated surface. In our previous work on the Pd/MgO system, two different Pd−Pd potentials were employed: one of them was extracted from the Pd_2 potential energy curve and the other from the interaction curve between a single Pd atom and an already adsorbed Pd center. Yet, it was shown that only the latter correctly reproduced the fcc structure observed in Pd clusters deposited on MgO.[36] According to these findings, in the present simulations, we have determined the Pd−Pd pair potential from the Pd−Pd(ads) potential energy curve where Pd(ads) stands for a Pd atom adsorbed on the Al terminated surface α-Al_2O_3 (0001). This procedure is not free from difficulties because the second Pd also feels the long-range surface electrostatic field. This contribution has to be removed from the Pd−Pd(ads) interaction energy. To avoid this double counting, such an electrostatic interaction has simply been removed out by using the Pd−O potential previously obtained. Finally, to ensure that the first derivative of the energy to be continuous at long distances (>10 Å), the $V_{ij}(s - r)$ contributions are multiplied by a smoothing function $f(r)$. The output of this procedure is an array V_{ij} $(r_1,r_2,r_3,...)$ of values representing the short-range contribution as reported in Figure 2.

The key pair potential in this kind of simulations obviously is the Pd−Pd one, which is why it will be briefly commented on here. As shown in Figure 2, the minimum of the curve occurs at an equilibrium Pd−Pd internuclear distance of 2.63 Å. This distance is slightly shorter than that found for the Pd−Pd(ads) potential used in the Pd/MgO system: 2.66 Å. The well depth

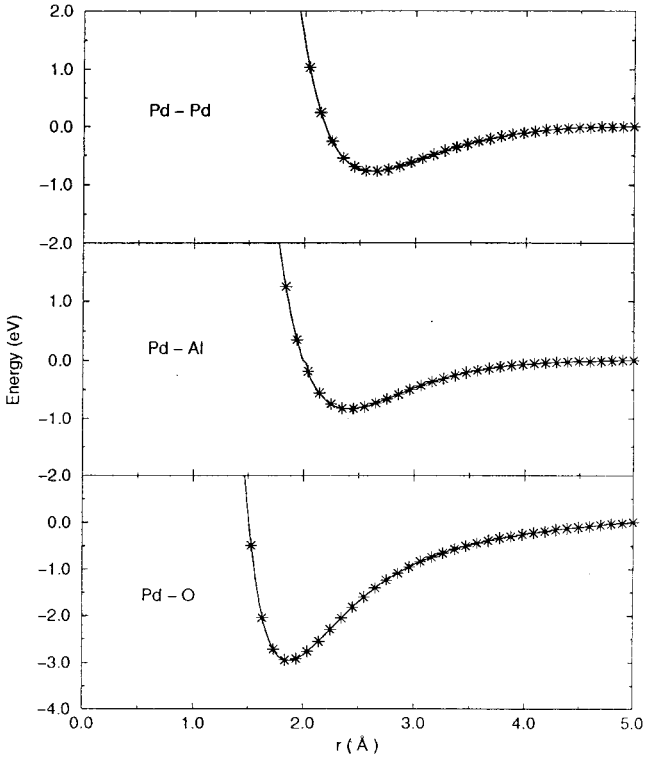

Figure 2. Interaction potentials for O−Pd, Al−Pd, and Pd−Pd pairs.

is also larger, 0.8 eV, for alumina, 0.6 eV, in the case of magnesia. These data reveal that the Pd−Pd potential for the alumina case is slightly stronger than that for magnesia, according to the fact that Pd atoms bind the alumina surface more efficiently (the adsorption energies are 1.41 eV for alumina[16] and ∼1 eV for magnesia[36,37]). Because the main contribution to the interaction energy arises from polarization of the Pd atoms, it clearly appears that Pd atoms adsorbed directly on the surface will be more polarized in the case of alumina. Therefore, Pd atoms bound to those that are directly adsorbed ones will be polarized to a larger extent, i.e., they will give rise to stronger interactions.

The behavior of this Pd−Pd potential was explored through some test MD simulations on two clusters of formula Pd_4 and Pd_6 for which ab initio B3LYP DFT calculations[39] have been reported. For Pd_4, a tetrahedral structure with Pd−Pd distances of 2.62 Å is obtained, whereas for Pd_6, our calculations lead to an almost perfect octahedron of 2.63 Å side. These distances reasonably agree with the mean values obtained from B3LYP DFT calculations: 2.657 and 2.713 Å for Pd_4 and Pd_6, respectively.

To get a deeper insight in to the Pd−surface interaction, local density of states for the Pd adsorbed on the Al and O terminated surfaces are reported in Figure 3 (top and bottom, respectively). Examination of DOS curves reveals the insulator character of the substrate and the almost neutral character of the adsorbed Pd atom. The calculated valence electron density plotted in Figure 4 provides further support to the local character of the interaction of Pd with the α-Al_2O_3 (0001) surface. This plot illustrates the largest interaction taking place between Pd and the O terminated surface. In this case, Pd atom lies closer to the surface, with well-defined isolines around Pd and O atoms.

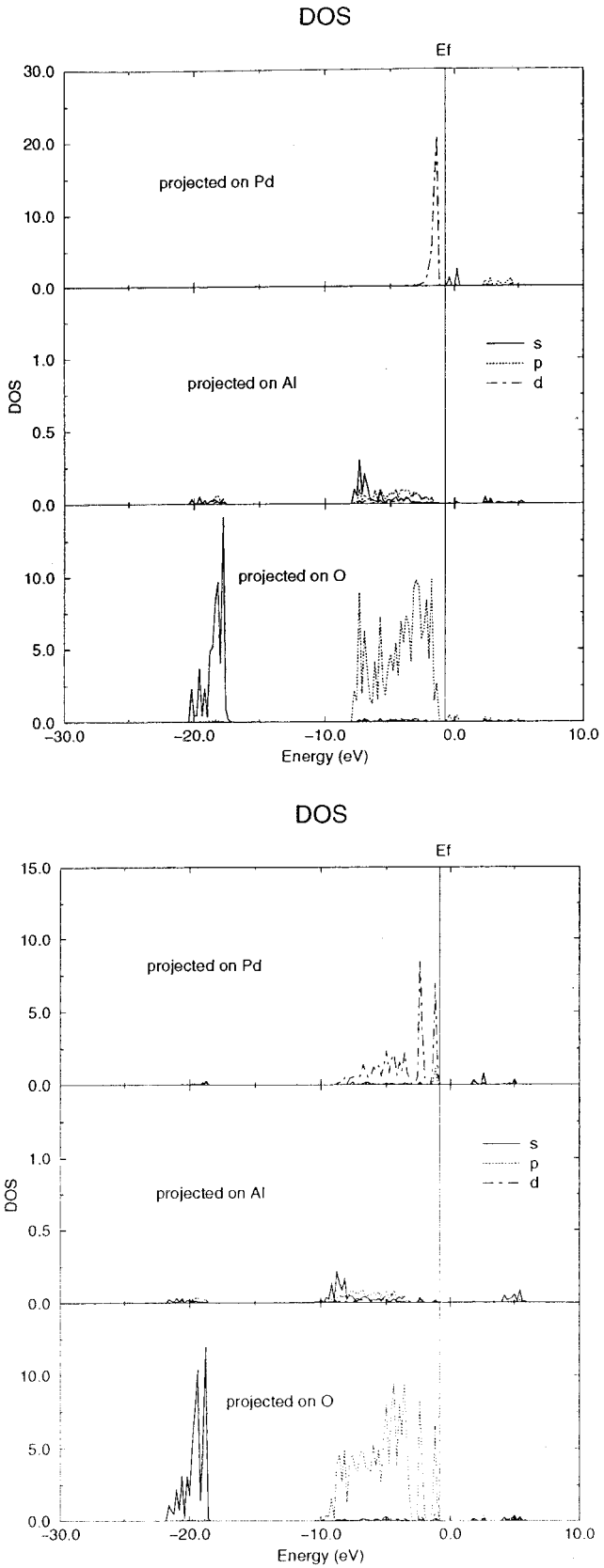

Figure 3. GGA density of states for $^1/_3$ ML of palladium adsorbed on Al_2O_3(0001) surface. Top, Al terminated surface; bottom, O terminated surface.

III. MD Simulations

Classical MD simulations were performed in the microcanonical ensemble using the DL_POLY computer code.[39] The computational box consisted of a (4 × 4 × 2) rhombic prism of α-Al_2O_3, which corresponded to a formula of $Al_{384}O_{576}$. The unit cell parameters used were those obtained from the DFT bulk calculations (a = 4.782 Å and c = 13.054 Å) which were

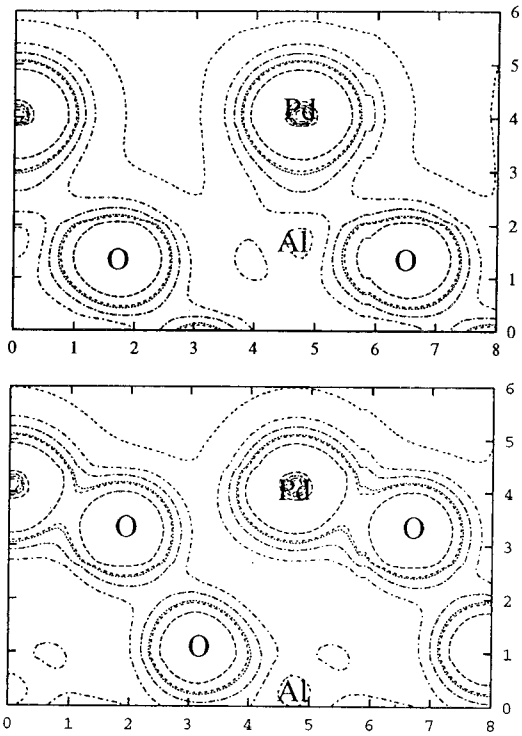

Figure 4. GGA valence electron density for $^1/_3$ ML of palladium adsorbed on $Al_2O_3(0001)$ surface. Top, Al terminated surface; bottom, O terminated surface.

found to be close to the experimental ones ($a = 4.760$ Å and $c = 12.995$ Å). Periodic boundary conditions in the three dimensions were used to mimic the infinite system with a vacuum gap of 75 Å in the ⟨0001⟩ direction used to define the alumina slab (~6 times the height of the larger deposited Pd cluster). These slabs are 36 layers thick; however, in the simulations, the 9 lowest layers were kept frozen. The long-range contributions were handled through the Ewald summation technique, and numerical integration was carried out using the leapfrog algorithm with a time step of 1 fs.

It is generally accepted that the most stable (0001) facet of native sapphire is Al terminated. Although this surface features large relaxation, which makes Al and O atoms almost in the same plane, it seems established from LEED experiments[41] that under ultrahigh vacuum conditions this is the favored termination. Therefore, the initial configuration in our MD simulations consisted of Pd clusters deposited on an Al terminated (0001) surface previously relaxed. Two different cluster sizes have been considered: 27 Pd atoms (a $3 \times 3 \times 3$ cube as starting point) and 64 Pd atoms ($4 \times 4 \times 4$); however, because the results obtained with the two clusters were essentially the same, only the largest cluster will be considered here. The initial configurations were allowed to relax in quite a large thermalization run (>100 ps) in which the velocities were rescaled. After a shorter run of 10 ps to verify if the system reached thermal equilibrium, another run of 50 ps was performed to obtain the data for statistics. The simulations were carried out at 300, 400, and 500 K, and the conservation of energy was better than 1 in 10 000.

Let us start the analysis with the simulations performed at low temperature, say $T = 300$ K. In Figure 5, a snapshot obtained at the end of the simulations is reported. It can be observed that beyond a certain degree of disorder the cluster exhibits a relatively well-defined shape, with a truncated pyramid like structure. With the aim of getting a deeper insight

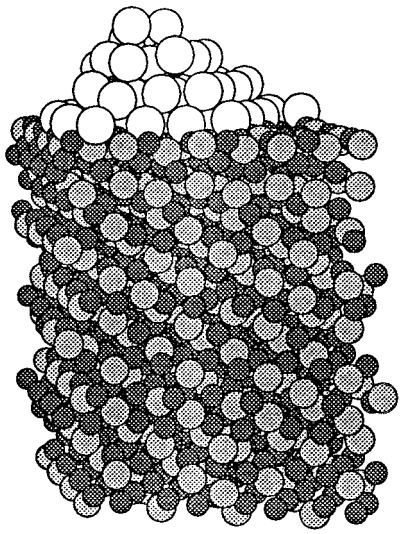

Figure 5. Snapshot of the Pd_{64} cluster deposited onto the $Al_2O_3(0001)$ surface at 300 K.

into the structure of this particle, an analysis of the Pd atom positions layer by layer was carried out. The results are displayed in Figure 6, where the projections along the (0001) direction of the surface, after progressive addition of consecutive Pd layers, are displayed. It should be noted that, with the aim of facilitating this analysis, the radii of the Pd atoms have been arbitrarily modified. The top of Figure 6 corresponds to the Pd layer directly adsorbed onto the alumina surface. It appears that there is quite a regular arrangement of Pd atoms showing an alignment with the surface oxygen rows, in particular, along (0,1,−1,0), (1,−1,0,0), and (0,0,1,0) directions. On the other hand, inner Pd atoms show a clear trend to reach a coordination number of six. This disposition leads to a layer with a more or less hexagonal shape with edges parallel to the mentioned azimuths. An additional aspect to highlight is the way in which the Pd rows are bound to the surface. Pd atoms always bind three oxygen atoms; however, because of the misfit of Pd and alumina lattices, both the surface alumina ions and the Pd adlayer atoms have to accommodate, with some extra surface relaxation. As shown in Figure 6, (middle) the second adlayer occupies the center of the first layer Pd triangles, according to both hexagonal and fcc packing. The third layer, bottom of Figure 6, confirms an A−B−C pattern according to cubic packing. The final structure could then be described as a hexagonal pyramid exposing (111) and (100) facets and truncated by the (111) plane. These findings are in excellent agreement with the STM images obtained under atomic resolution showing the regular structure of deposited Pd particles.[8] In Figure 7, the radial distribution functions, $g(r)$, for the Pd−O, Pd−Al, and Pd−Pd pairs are reported. The first feature of the Pd−Pd $g(r)$ consists of a broad band which reflects the fact that the Pd−Pd interlayer distances are relatively different. The maximum appears to be at 2.49 Å, which represents a contraction of about 5% with respect to the minimum observed in the Pd−Pd pair potential curve. The extent of this reduction agrees with the lattice constant contraction observed in small cluster (12 Å) as found from transmission electron microscopy of Pd particles supported on Al_2O_3 films.[42,43]

A further interesting point refers to the work of adhesion of Pd particles supported on alumina. Using the STM data of Pd deposited on a thin film of Al_2O_3 growth on NiAl(110), Hansen et al. reported a work of adhesion of 2.8 ± 0.2 J/m^2. Recent calculations reported by Bogicevic and Jennison[15] on Pd adsorption atop a 5 Å thick aluminum oxide film on Al(111)

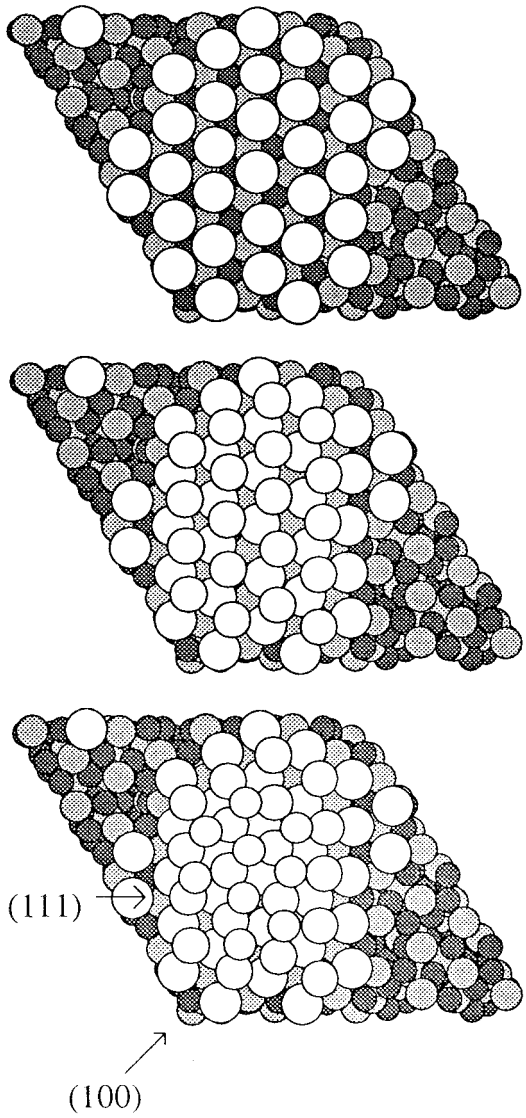

Figure 6. Layer by layer views of the Pd_{64} cluster deposited onto the $Al_2O_3(0001)$ surface.

give values of 1.7 J/m^2 for a full monolayer using the LDA local density approximation. For coverage of 4 ML, the work of adhesion raises to 1.95 J/m^2, whereas when the GGA functional is used, this value drops to 1.05 J/m^2. The hypothetical reasons for the discrepancy between quantum mechanical estimates and experimental adhesion energies for this surface have been discussed at some length by these authors elsewhere.[44] Concerning the (0001) surface of native sapphire, and as stated above, using the GGA exchange correlation functional and the same surface and computational approach described in the present work,[16] the adsorption energy for $^1/_3$ coverage was found to be 1.41 eV. However, this value has to be corrected because, to compare with cluster model calculations, this adsorption energy was computed using as reference an isolated Pd atom instead of a pseudomorphic Pd overlayer.[45] The correction diminishes the adhesion energy by roughly 0.1 eV, giving rise to a final value of 1.06 J/m^2. This value appears to be significantly lower than that obtained from the aluminum oxide film on Al(111), although the comparison is not straightforward because both support and coverage are different. To facilitate the comparison, the adhesion energy for 1 ML coverage was computed from GGA calculations in the present work. The estimated adhesion energy *per* atom at this coverage is 0.48

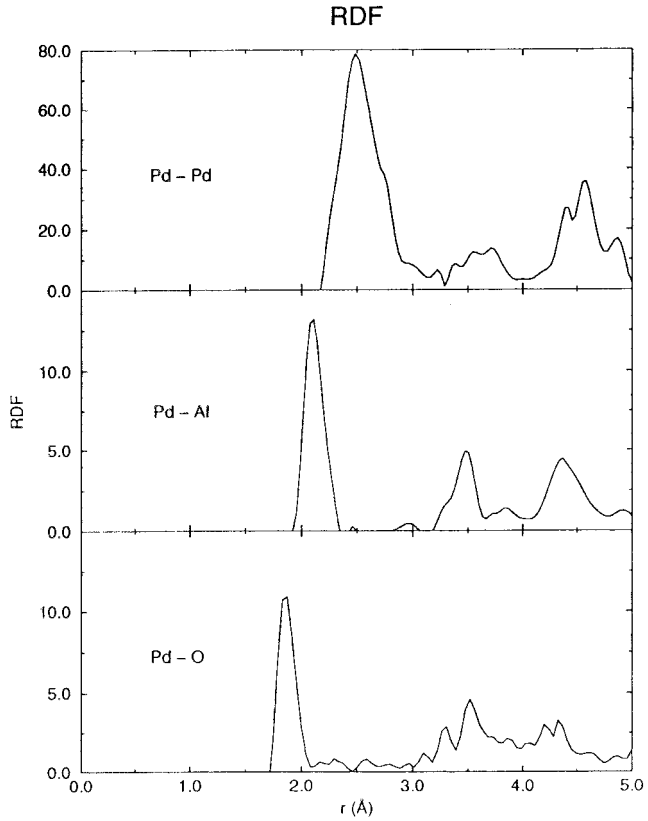

Figure 7. Radial distribution functions, RDF, for Pd−Pd, Pd−Al, and Pd−O pairs obtained from MD simulations at 300 K.

eV or 0.39 J/m^2. Compared to the LDA calculations mentioned above, our GGA adhesion energies appear to be clearly lower, indicating some dependence of this quantity on the structure of the support. It should be noted that GGA adhesion energies have been found to be lower than LDA ones in related systems;[44] however, the differences in the present case seem to be too large for being only ascribed to the theoretical approach. Moreover, our GGA 1 ML adhesion energy is also found lower than that found for a 2 ML coverage from LDA calculations: 1 eV. Finally, another interesting point is that on going from $^1/_3$ to 1 ML coverage, a decrease in the adhesion energy is observed. This lowering in the binding agrees with that observed in related systems such as Pt/α-Al_2O_3[35] and indicates that, on increasing coverage, the Pd overlayer is recovering its metallic character.

We will explore here the predictions issued from MD classical simulations. Using the configuration energies obtained from the simulations, this quantity is estimated to be 3.1 J/m^2, in reasonable agreement with the experiment. This agreement can be accounted for taking into account that upon adsorption of Pd clusters there is a deep surface relaxation in which the Al atoms move inward, and therefore, the surface almost corresponds to an oxygen-terminated surface. However, the interaction energy of Pd atoms with the oxygen-terminated surface is significantly larger. In particular, the adsorption energy at $^1/_3$ ML computed for the on top of oxygen sites is 2.96 eV (this value corresponds to the height of the Pd−O potential in Figure 2), which is more than twice that computed for the Al terminated surface.

The supported clusters are relatively stable and maintain a 3D morphology at moderate temperatures: 300 and 400 K, even in long simulation runs. However, when the temperature is increased to 500 K, they get unstable, and after a few picoseconds, some of the Pd atoms penetrate into the surface, starting a process in which the surface cluster is destroyed. A

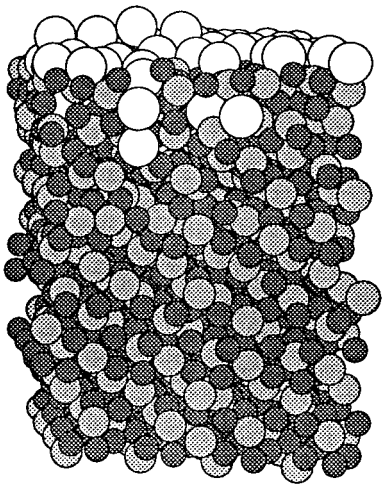

Figure 8. Snapshot of the Pd_{64} cluster deposited onto the $Al_2O_3(0001)$ surface obtained at 500 K showing the diffusion of Pd into the bulk.

snapshot of this situation obtained after a simulation of the system at 500 K for 20 ps is shown in Figure 8. As can be seen, there is a diffusion of Pd atoms into the metal oxide support, which at the end gives rise to the disappearance of the catalyst from the surface. Such diffusion agrees with the interpretation proposed for the loss of surface activity observed from experiments that have clearly demonstrated that the surface activity of $Pd/Al_2O_3/NiAl(110)$ decreases upon heating the system.[17] A similar Pd diffusion into the support and subsequent formation of Pd−Al alloy has also been observed for thick Pd−Al_2O_3/Al interfaces using XPS and XAES techniques.[18] From a careful analysis of the crucial configurations, we can track the first steps of Pd penetration into the surface. The initial step is an in phase movement of three surface oxygen atoms under which there is one of the pseudo-octahedral holes of the α-Al_2O_3 surface. This allows single Pd atoms to move and to occupy these holes, producing a significant perturbation of the neighboring Al−O polyhedrons. Such distortions permit new Pd atoms to move inward and to diffuse in a relatively easy and quick way. After diffusion, the Pd coordination is found to be somewhat heterogeneous. As shown in Figure 9 where two cross sections are displayed, Pd is surrounded by both Al and O atoms and there are some Pd dimers too. Yet, although one could expect that Pd atoms would try to reach their maximal coordination with oxygen atoms, we think that the alumina slab used here is not thick enough to allow for the reaching of this ideal situation.

IV. Conclusions

In this work, classical MD simulations of Pd clusters deposited on the α-Al_2O_3 (0001) surface are reported. With the aim of avoiding possible bias derived from the use of empirical force fields, the potential functions used to describe the metal−surface interaction were derived on a purely a priori basis from supercell periodic DFT calculations using a GGA exchange correlation functional and plane waves as basis set. The simulations show that the adsorbed Pd particles are 3D clusters supporting the 3D Volmer−Weber growth mechanism suggested for this system. The structural analysis unambiguously shows the cubic packing of the microcrystals whose shape appears to be hexagonal pyramids truncated by the (111) plane and exhibiting (111) and (100) facets. These results are in excellent agreement with the STM images reported by Hansel et al.[8] The supported particles are stable at low and moderate temperatures; however, when the simulations are performed at 500 K, Pd

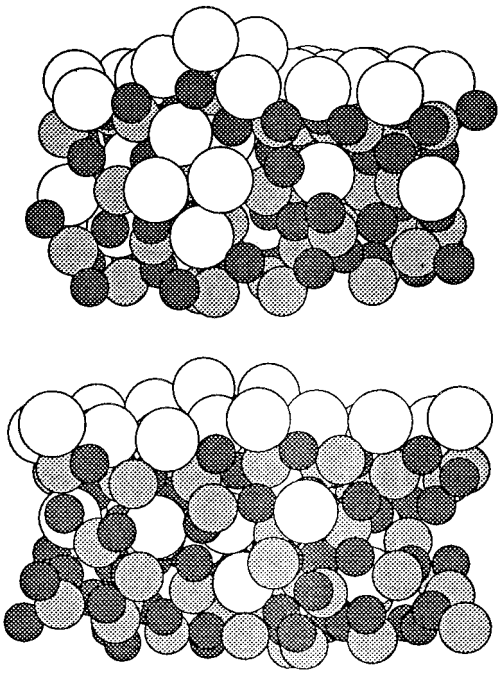

Figure 9. Two cross-sections of the configuration displayed in Figure 8, showing the coordination of inner Pd atoms.

atoms tend to penetrate into the bulk, leaving the surface. Although the performance of our classical MD simulations is limited, this diffusion agrees with the loss of surface activity experimentally observed when the temperature of the $Pd/Al_2O_3/NiAl(110)$ catalytic system is increased,[17] as well as with XPS and XAES data.[18]

Acknowledgment. Financial support from the Spanish DGESIC, Project PB98-1125, is fully acknowledged. N.C.H thanks the Junta de Andalucía for a predoctoral grant (Project FQM132). This work was partially reported at the Euresco conference of Molecular Mechanisms of Heterogeneous Catalysis held in San Feliu de Guixols, Spain, June 23-28, 2001. We thank the participants, in particular Dr. J. Libuda, for helpful discussions.

References and Notes

(1) Goodman, D. W. *Chem. Rev.* **1995**, *95*, 523.
(2) Gates, B. C. *Chem. Rev.* **1995**, *95*, 511.
(3) *Chemisorption and Reactivity on Supported Clusters and Thin Films: Towards an Understanding of Microscopic Processes in Catalysis*; Lambert, R. M., Pacchioni, G., Eds.; Kluwer: Dordrecht, The Netherlands, 1997.
(4) Jaeger, R.; Kuhlenbeck, H.; Freund, H.-J.; Wuttig, M.; Hoffmann, W.; Franchy, R.; Ibach, H. *Surf. Sci.* **1991**, *259*, 235.
(5) Libuda, J.; Winkelmann, F.; Bäumer, M.; Freund, H.-J.; Bertrams, Th.; Neddermeyer, H.; Müller, K. *Surf. Sci.* **1994**, *318*, 61.
(6) Bäumer, M.; Libuda, J.; Freund, H.-J. In *Chemisorption and Reactivity on Supported Clusters and Thin Films: Towards an Understanding of Microscopic Processes in Catalysis*; Lambert, R. M., Pacchioni, G., Eds.; Kluwer: Dordrecht, The Netherlands, 1997; p 61.
(7) Bäumer, M.; Libuda, J.; Freund, H.-J. *Prog. Surf. Sci.* **1999**, *61*, 127.
(8) Hansen, K. J.; Worren, T.; Stempel, S.; Laegsgaard, E.; Bäumer, M.; Freund, H.-J.; Besenbacher, F.; Stensgaard, I. *Phys. Rev. Lett.* **1999**, *83*, 4120.
(9) Dellwig, T.; Hartmann, J.; Libuda, J.; Meusel, I.; Rupprechter, G.; Unterhalt, H.; Freund, H.-J. *J. Mol. Catal. A* **2000**, *162*, 51.
(10) Libuda, J.; Meusel, I.; Hoffmann, J.; Hartmann, J.; Piccolo, L.; Henry, C. R.; Freund, H.-J. *J. Chem. Phys.* **2001**, *114*, 4669.
(11) Watanabe, K.; Matsumoto, Y.; Kampling, M.; Al-Shamery, K.; Freund, H.-J. *Angew. Chem., Int. Ed.* **1999**, *38*, 2192.
(12) Bruna, J. C.; Gillet, M.; Gonzales, V.; Masek, K.; Matolin, V. *Surf. Rev. Lett.* **1998**, *5*, 403.

(13) Nehasil, V.; Zafeiratos, S.; Matolin, V.; Ladas, S. *Vacuum* **1998**, *50*, 143.
(14) Pang, C. L.; Raza, H.; Haycock, S. A.; Thornton, G. *Surf. Sci.* **2000**, *460*, L510.
(15) Bogicevic, A.; Jennison, D. R. *Phys. Rev. Lett*. **1999**, *82*, 4050.
(16) Gomes, J. R. B.; Illas, F.; Hernández, N. C.; Márquez, A.; Sanz, J. F. *Phys. Rev. B* in press.
(17) Sandell, A.; Libuda, J.; Bäumer, M.; Freund, H.-J. *Surf. Sci*. **1996**, *346*, 108.
(18) Sarapatka, T. *J. Phys. Chem.* **1993**, *97*, 11274.
(19) Car, R.; Parrinello, M. *Phys. Rev. Lett.* **1985**, *55*, 2471.
(20) Oviedo, J.; Calzado, C. J.; Sanz, J. F. *J. Chem. Phys*. **1998**, *108*, 4219.
(21) Oviedo, J.; Sanz, J. F.; López, N.; Illas, F. *J. Phys. Chem. B* **2000**, *104*, 4342.
(22) Lewis, G. V.; Catlow, C. R. A. *J. Phys. C: Solid State Phys.* **1985**, *18*, 1149.
(23) San Miguel, M. A. Ph.D. Thesis, University of Sevilla, Sevilla, Spain, 1998.
(24) Baxter, R.; Reinhardt, P.; López, N.; Illas, F. *Surf. Sci*. **2000**, *445*, 448.
(25) Guenard, P.; Renaud, G.; Barbier, A.; Gautier-Soyer, M. Proceedings ICSOS, Aix en Provence, 1996.
(26) Mackrodt, W. C. *J. Chem. Soc., Faraday Trans 2* **1989**, *85*, 541.
(27) Mackrodt, W. C. *Philos. Trans. R. Soc. London* **1992**, *A341*, 301.
(28) Manassidis, I.; Gillan, M. J. *J. Am. Ceram. Soc*. **1994**, *77*, 335.
(29) Blonski, S.; Garofallini, S. H. *Surf. Sci*. **1993**, *295*, 263.
(30) Kresse, G.; Hafner, J. *Phys. Rev B* **1993**, *47*, 558.
(31) Kresse, G.; Furthmüller, J. *Comput. Mater. Sci*. **1996**, *6*, 15.
(32) Kresse, G.; Furthmüller, J. *Phys. Rev. B* **1996**, *54*, 11169.
(33) Perdew, J.; Chevary, J.; Vosko, S.; Jackson, K.; Pederson, M.; Singh, D.; Fiolhais, C. *Phys. Rev. B* **1992**, *46*, 6671.
(34) Vanderbilt, D. *Phys. Rev. B* **1990**, *41*, 7892.
(35) Verdozzi, C.; Jennison, D. R.; Schultz, P. A.; Sears, M. P. *Phys. Rev. Lett*. **1999**, *82*, 799.
(36) Henry, C. R.; Chapon, C.; Duriez, C.; Giorgio, S. *Surf. Sci*. **1991**, *253*, 177.
(37) López, N.; Illas, F. *J. Phys. Chem. B* **1998**, *102*, 1430.
(38) Henry, C. R.; Meunier, M.; Morel, S. *J. Cryst. Growth* **1990**, *129*, 416.
(39) Valerio, G.; Toulhoat, H. *J. Phys. Chem*. **1996**, *100*, 10827.
(40) Smith, W.; Forester, T. R.; Daresbury Laboratory, 1995.
(41) Toofan, J.; Watson, P. R. *Surf. Sci*. **1998**, *401*, 162.
(42) Nepijko, S. A.; Klimenkov, M.; Adelt, M.; Kuhlenbeck, H.; Schlögl, R.; Freund. H.-J. *Langmuir* **1999**, *15*, 5309.
(43) Klimenkov, M.; Nepijko, S. A.; Adelt, M.; Kuhlenbeck, H.; Bäumer, M.; Schlögl, R.; Freund. H.-J. *Surf. Sci.* **1997**, *391*, 27.
(44) Jennison, D. R.; Bogicevic, A. *Surf. Sci*. **2000**, *464*, 108.
(45) The adsorption energy in ref 16 was $E_{ad} = E_{slab} - E_{support} - E_{metal}$, where E_{slab} stands for the energy of optimized the $Pd-Al_2O_3$ slab, $E_{support}$ for the energy of the optimized alumina slab, and E_{metal} for the energy of an almost free Pd atom (actually a monolayer of Pd atoms 10 Å apart). In the present context, it seems more coherent to use as reference the energy of a Pd overlayer calculated with a lattice pseudomorphic to that of the support.